

Detection of residual free radicals in tomato juice processed by stand-alone and combined ultrasonic and ultraviolet treatments

Kristina Smokrović^{a,#}, Sanda Pleslić^{b,#}, Franka Markić^a, Senada Muratović^a, Tomislava Vukušić Pavičić^c, Višnja Stulić^c, Manuela Zadravec^d, Nadica Maltar-Strmečki^{a,*}

^a Ruder Bošković Institute, Bijenička c. 54, Zagreb, 10000, Croatia

^b University of Zagreb Faculty of Electrical Engineering and Computing, Unska 3, Zagreb, Croatia

^c University of Zagreb Faculty of Food Technology and Biotechnology, Laboratory for Food Processes Engineering, Pierottijeva 6, Zagreb, Croatia

^d Croatian Veterinary Institute, Savska c. 143, Zagreb, 10000, Croatia

ARTICLE INFO

Keywords:

Food processing
UV-A irradiation
Ultrasound processing
EPR spectroscopy
Free radicals
Antioxidant, Tomato juice

ABSTRACT

This study investigated the effects of ultraviolet-A (UV-A), ultrasound (US), and combined UV-A/US treatments on bioactive compounds, antioxidant activity, and free radical generation in tomato pulp. Individual bioactive compounds responded differently to UV-A, US, and combined UV-A/US treatments, depending on treatment conditions and number of cycles. The highest total polyphenol content (TPC) was obtained under UV-A irradiation at 50 mW in the third treatment cycle (224.71 mg/L GAE), while lycopene and beta-carotene reached their maximum concentrations under UV-A at 100 mW (1.287 µg/mL and 0.286 µg/mL, respectively). The highest reduction of the EPR–DPPH signal was observed under combined UV-A/US treatment (31.49 %), whereas the US treated sample (60 % of amplitude) showed the lowest reduction (15.12 %). CMH spin trapping measurements showed that CP equivalents increased with treatment intensity and number of cycles, with the highest CP value (73.72 µmol/L) obtained under ultrasound treatment at 90 % amplitude after three cycles. UV-A treatment alone resulted in lower CP values, which increased gradually with higher irradiation power and additional cycles.

1. Introduction

Tomatoes are among the most widely consumed vegetables in the Western world, with products such as sauces, juices, and pastes ubiquitous on the market (Ali et al., 2021; Bal et al., 2024; Basdemir et al., 2024). Fresh tomatoes are rich in valuable bioactive compounds, including L-ascorbic acid, lycopene, beta-carotene, phenolic compounds, proteins, monounsaturated fatty acids, dietary fiber, and various minerals (Ali et al., 2021). To minimize the loss of these compounds during processing and storage, it is essential to limit microbial activity, exposure to oxygen, and the action of endogenous enzymes such as polyphenol oxidase (Spagna et al., 2005). These enzymes can be inactivated by thermal, irradiation, or pressure-based methods (Li et al., 2023; Zawawi et al., 2022).

With the growing popularity of the Mediterranean diet, there is

increasing demand for novel processing technologies that preserve or enhance nutrient and bioactive compound content in fruits and vegetables (Ates et al., 2025; Guasch-Ferré & Willett, 2021). Non-thermal processing methods, in particular, have gained attention because they minimize degradation of heat-sensitive compounds by maintaining low treatment temperatures and using short processing times (Barbosa-Cánovas et al., 2022; Jiménez-Sánchez et al., 2017a, 2017b). Treatments such as ultraviolet (UV) irradiation or gamma radiation induce biocidal effects primarily through chemical disruption of microbial membranes via the generation of transient free radicals, while high-pressure homogenization and ultrasound (US) achieve similar effects through physical mechanisms such as pressure fluctuations and cavitation (Cheng et al., 2020; Cui et al., 2022; Giulitti et al., 2011; Mason et al., 1994; Petrier et al., 1992). In the case of US, cavitation leads to the formation of reactive oxygen and nitrogen species (ROS and

* Corresponding author.

E-mail addresses: kristina.smokrovic@irb.hr (K. Smokrović), sanda.pleslic@fer.unizg.hr (S. Pleslić), fmarkic@irb.hr (F. Markić), Senada.Muratovic@irb.hr (S. Muratović), visnja.stulic@pbf.unizg.hr (T.V. Pavičić), tomislava.vukusic.pavicic@pbf.unizg.hr (V. Stulić), zadravec@veinst.hr (M. Zadravec), nstrm@irb.hr (N. Maltar-Strmečki).

Authors equally contributed to the research and share first authorship.

<https://doi.org/10.1016/j.afres.2026.101988>

Received 3 September 2025; Received in revised form 27 February 2026; Accepted 8 April 2026

Available online 9 April 2026

2772-5022/© 2026 The Author(s). Published by Elsevier B.V. This is an open access article under the CC BY-NC license (<http://creativecommons.org/licenses/by-nc/4.0/>).

RNS), which can also interact with plant cell walls and membranes, enhancing the release and bioavailability of bioactive compounds (Anbar et al., 1966; Colle et al., 2013; Li et al., 2016; Lopez-Sanchez et al., 2011; Mehta et al., 2019; Yanagida et al., 1999). Recent research highlights that processing conditions, including ultrasound power and treatment cycles, significantly affect the retention of bioactive compounds, antioxidant activity, and microbial characteristics in beverage matrices (Noorisefat et al., 2025).

Electron paramagnetic resonance (EPR) spectroscopy is a powerful tool for detecting species with unpaired electrons, as its measurements are unaffected by sample turbidity or optical absorption. Reagents such as CMH rapidly and efficiently trap oxidative radicals, forming stable CM• products that can be directly quantified by EPR (Dikalov et al., 2011; Gotham et al., 2020). This approach enables assessment of total CMH-reducible oxidants, including both primary radicals and secondary intermediates such as RNOS generated from H₂O₂, providing a net insight into oxidative activity in complex food matrices (Bagryanskaya et al., 2015; Gotham et al., 2020; Khan et al., 2003). ROS are generally short-lived species, with the exception of hydrogen peroxide and organic peroxides, which have half-lives of 1–1000 ns even in the absence of antioxidants (Rubio & Cerón, 2021; Sies et al., 2017). The combination of UV-A and US treatments can result in complex interactions, where UV-A alters the kinetic steady state of free radicals generated during sonication, potentially producing synergistic or antagonistic effects on oxidative activity (Akti & Yildiz, 2025; Ashokkumar, 2011; Buxton et al., 1988; Trinh et al., 2025; Yikmis et al., 2025).

In the present study, we investigated the effects of UV-A and US treatments, individually and in combination (UV-A/US), on the residual concentration of free radicals in tomato juice and their impact on physicochemical and microbial properties. To our knowledge, the residual radicals produced under these treatment conditions across three treatment cycles were analyzed for the first time using CMH spin-trapping and EPR spectroscopy. We further evaluated the influence of treatment parameters, including UV-A power, US amplitude, and number of cycles, on radical concentration. An essential aspect of introducing novel processing technologies, particularly in combination, is understanding their potential synergistic or antagonistic effects. Accordingly, we also report results for total soluble solids, pH, titratable acidity, phenol and carotenoid content, DPPH antioxidant activity, and microbiological characteristics.

2. Materials and methods

2.1. Tomato juice preparation

Ripe plum tomatoes (*Solanum lycopersicum* L., cultivar “Roma”) were purchased from the Croatian organic farm “Vrtni centar Baković”, Holus d.o.o., Sveti Filip i Jakov, Croatia (latitude: 43.97277, longitude: 15.41523, 2022). The tomatoes were washed with cold water immediately before processing. The peel was removed using the hot-break method (95 °C, 30 s, followed by an ice bath). The peeled tomatoes were cut into pieces, and the seeds were separated using a sieve. The remaining pulp was homogenized, filtered and tomato juice samples were prepared by mixing 70 % supernatant and 26 % of the filtration residue to total volume of 150 mL. The tomato juice samples were stored in plastic cups at –20 °C until further analysis.

2.2. Ultrasonic and ultraviolet treatment

All samples were cooled to 7 °C and pre-treated with a mechanical homogenizer (Omni GLH 850 General Laboratory Homogenizer, Omni International, Inc, Kennesaw GA, USA) for 3 min at 10 000 rpm. The homogenized sample (150 mL) was transferred into a 250 mL, quartz round flask equipped with a stirring magnet.

The samples were then treated with UV-light (365 nm) and/or ultrasonic waves using a 27.8 kHz ultrasound generator (Fig. 1) with a 14 mm diameter probe. Technical details are provided in Table S1a and S1b, SI. Simultaneously, the ultrasonic probe was immersed 5 cm into the sample. One treatment cycle consisted of 5 min of UV-light irradiation, with 1 min of ultrasonic processing during the 3rd minute of irradiation. The samples were subjected to one, two or three treatment cycles, with three repetitions and constant mechanical stirring at 150 rpm. During the ultrasonic treatment, the probe immersed in the reaction mixture continuously monitored the bulk temperature, which did not exceed 40 °C. All laboratory equipment used for sample handling was sterilised by autoclaving with steam, except for the ultrasonic probe and the mechanical homogeniser, which were sterilised with 96 % ethanol. The centrifuge tubes used for sample collection after treatment were purchased pre-sterilised and used as is (LLG Labware centrifuge tubes 15 mL, Lab Logistics group GmbH, Meckenheim, Germany). After treatment, the sample was divided into 10 mL aliquots, which were used

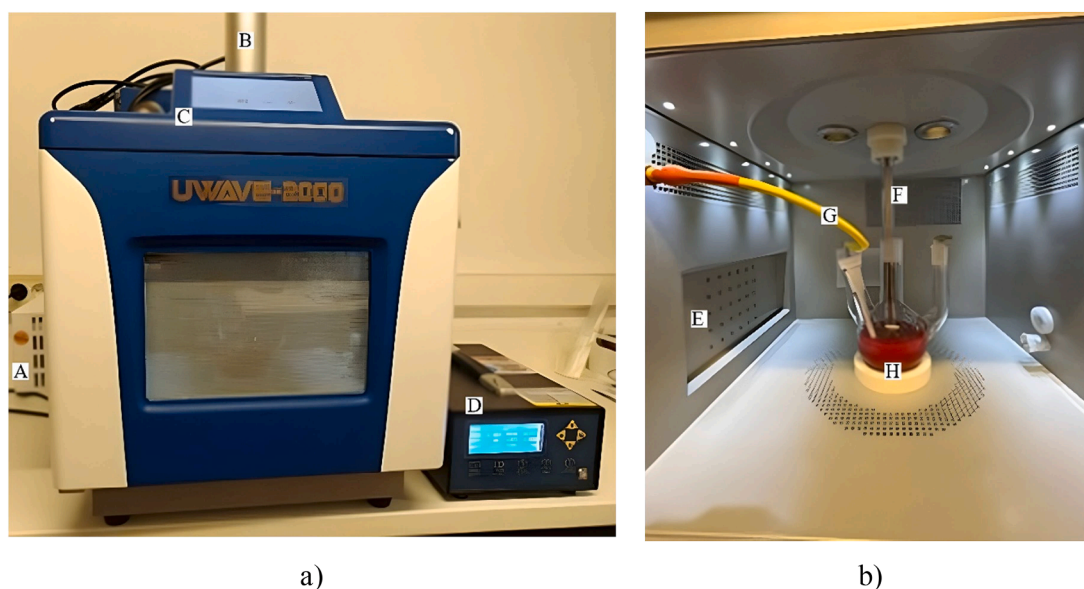


Fig. 1. UWave 2000 multipurpose microwave chemistry workstation (Shanghai SineoMicrowave Chemistry Technology Co., Ltd., Jinan, Shan-dong Province, China) a) Front view and b) Interior view, showing the following accessories attached: A - UV lamp 365 nm, B - ultrasonic probe holder, C - workstation control panel, D - ultrasonic generator, E - UV-A output, F - ultrasonic probe, G - temperature sensor, H - magnetic stirrer.

for further characterisation analyses. The aliquots were stored at 4 °C in sterile centrifuge tubes until further analysis.

2.3. Electron paramagnetic resonance (EPR) spin-trapping spectroscopy

The spin trapping was accomplished by 1-hydroxy-3-methoxycarbonyl-2,2,5,5-tetramethylpyrrolidine (CMH) purchased from Noxygen Science Transfer & Diagnostics GmbH, Elzach, Germany. CMH is used as a spin probe in EPR experiments to detect reactive oxygen species, primarily superoxide radicals, by forming a stable nitroxide radical (CM•) measurable by EPR spectroscopy. Chemical structure and description of CMH spin probe is given in SI, Figure S1. Stock solution of the spin probe (CMH, concentration 1.0 mol/L) was prepared using a citrate buffer (0.100 mol/L, pH = 4.4), deferoxamine mesylate (DFAM, 5 µmol/L) and sodium diethyldithiocarbamate trihydrate (DETC, 25 µmol/L) continuously de-oxygenated by nitrogen gas to maintain minimal background oxidation of the spin traps.

Citric acid buffer was prepared from citric acid monohydrate and anhydrous sodium carbonate purchased from Kemika d.d., Zagreb, Croatia, using Milli-Q® water. DFAM and DETC were purchased from Noxygen Science Transfer & Diagnostics GmbH, Elzach, Germany. CMH stock solution (1.0 mol/L) was immediately divided into centrifuge tubes (10 µL aliquots), purged with nitrogen and kept in the dark at –20 °C until use. Immediately after each treatment, a 150 µL aliquot of sample was added to the prepared stock solution of CMH (total volume 160 µL). After incubation in the dark for 30 min, a 50 µL was immediately transferred into the BLAUBRAND® disposable intraMark micropipettes (Brand GmbH, Wertheim am Main, Germany). EPR spectra were recorded at 150 K using benchtop Bruker Magnetech ESR5000 spectrometer (Bruker BioSpin, Rheinstetten, Germany) operating at X-band frequency (approx. 9.5 GHz) and using a flow of cold nitrogen gas for temperature control. EPR conditions were as follows: microwave power, 5 mW, magnetic field modulation amplitude 0.3 mT, modulation frequency 100 kHz, sweep width 20 mT.

The control spectra (160 µL), consisting of only Milli-Q® water (150 µL) and the CMH (10 µL), showed no EPR signal. Spectra analysis were done using ESR Studio v. 1.80.0 (Bruker BioSpin, Rheinstetten, Germany). The peak-to-peak amplitude (A_{pp}) of the central EPR spectral line after baseline correction via background subtraction was evaluated for determination of residual radical concentration. The concentration of free radicals generated during processing were calculated using a CP free radical presented in Figure S1, SI (Noxygen Science Transfer & Diagnostics GmbH, Elzach, Germany). The CP free radical is used to create a calibration curve, by which the intensity of the EPR signal (peak-to-peak amplitude) is converted into the absolute spin concentration (Figure S2, SI). The calibration curve (1.25–100 µmol/L) of CP free radical Figure S3, SI was prepared by dissolving CP in the citrate buffer (0.100 mol/L, pH=4). The free radical concentrations in tomato juice samples are expressed as CP equivalents (CPE µmol/L)

2.4. Physicochemical characterization

2.4.1. pH, titratable acidity and total soluble solids

pH and titratable acidity (TA) were determined using Orion STAR 211 pH-meter (Thermo Fisher Scientific Inc., Waltham, Massachusetts, SAD) using the ROSS-electrode and Orion™ pH Buffer solutions (pH values 4.01, 7.00 and 10.01) were used for instrument calibration. For TA determination, 1.00 ml of the tomato juice sample was added to 10.00 mL of Milli-Q® water and sodium hydroxide solution Titripur® (Sigma-Aldrich, Schnellendorf, Germany) was used for titration (10.0 mmol/L). TA is expressed as percentage (%) of citric acid equivalent.

Total soluble solids (TSS) were determined by an automated refractometer and expressed in Brix degrees (°Brix) using a digital refractometer (MA885 Digital Refractometer, Milwaukee Instruments, Rocky Mount, North Carolina, SAD Milli-Q® water was used for refractometer calibration.

2.4.2. The Folin-Ciocalteu (FC) method for determination of total polyphenol content (TPC)

Total polyphenol content (TPC) of the treated tomato samples was determined according to the modified method described by Kupina et al. (Kupina et al., 2018). An aliquot of 50.0 µL of the tomato sample was added to 2.97 ml of Milli-Q® water, followed by 250.0 µL of the Folin-Ciocalteu (FC) reagent (Sigma-Aldrich, Schnellendorf, Germany). The solution was vortex stirred for one minute, and after 15 min, 500 µL of aqueous sodium carbonate solution (20 % w/w) was added and the solution was incubated at 60 °C in the dark for 1 hour after which absorbance was measured at 765 nm using spectrophotometer Giorgio Bormac s.r.l., Carpi, Italy. The concentration of total polyphenol compounds in tomato juice samples was calculated using gallic acid (Thermo Scientific™ Chemicals, Waltham, Massachusetts, SAD) calibration curve (0–500 mg/L), and results are expressed as gallic acid equivalents (GAE mg/L).

2.4.3. Carotenoids

The carotenoids, lycopene and beta-carotene, were extracted according to a modified method described by Nagata et al. (Nagata & Yamashita, 1992). After the treatments, samples were divided in aliquots (0.10 mL) which were placed in the plastic tubes and filled up with 1 mL of 4:6 v/v acetone:n-hexane solution. Acetone was purchased from Kemika d.d., Zagreb, Croatia while n-hexane was purchased from VWR Chemicals, Radnor, Pennsylvania, SAD. Prepared suspension was vortexed for 15 min at 3000 rpm and centrifugated. Supernatant was divided from precipitate and extraction was repeated one more time. After extraction, obtained supernatants were mixed and stored in sealed tubes at 4 °C until analysis, which was performed within 2 h of extraction. The instrument was calibrated before the measurement with a suitable cuvette filled with an acetone/hexane mixture (4:6 v/v). The absorbances were measured using spectrophotometer Giorgio Bormac s. r.l., Carpi, Italy at 453, 505, 645 and 663 nm and concentration of lycopene and beta-carotene were calculated according to equations (Nagata & Yamashita, 1992):

$$C_{lyc} = -0.0458 A_{663} + 0.204 A_{645} + 0.372 A_{505} - 0.0806 A_{453} \quad (1)$$

$$C_{betac} = 0.216 A_{663} - 1.22 A_{645} - 0.304 A_{505} + 0.452 A_{453} \quad (2)$$

where A_{663} , A_{645} , A_{505} , and A_{453} correspond to absorbance at 663, 645, 505, and 453 nm, respectively. The lycopene and beta-carotene concentrations are expressed in µg/mL.

2.4.4. Total antioxidant activity

The antioxidant activity was determined using the DPPH assay (Brand-Williams et al., 1995). A stock solution was prepared with 19.71 mg DPPH (Sigma-Aldrich, Schnellendorf, Germany) and 500.00 mL of 96 % ethanol (Gram-Mol, Zagreb, Croatia) in a volumetric flask, resulting in a 0.100 mmol/L solution. The prepared solution was wrapped in aluminium foil, aerated for 15 min under a steady stream of nitrogen gas and stored overnight in a refrigerator at 4 °C. In triplicate, 20.0 µL of the sample was added to 5.00 mL of DPPH stock solution. The solution was stirred well and covered with aluminium foil for 1 hour at 21 °C.

The EPR spectra were collected using Bruker Magnetech ESR5000 spectrometer (Bruker BioSpin, Rheinstetten, Germany) at X-band frequency and at room temperature. The following instrument parameters were used: microwave power, 4 mW, magnetic field modulation amplitude 0.2 mT, modulation frequency 100 kHz and sweep width 12 mT. Each spectrum presents an average of five accumulations. The DPPH solutions were analysed using calibrated micropipettes (Brand GmbH, Wertheim am Main, Germany) of a fixed diameter and filled to the 50 µL mark. The micropipettes were sealed with critoseal. In EPR spectroscopy, the concentration of detected unpaired electrons (in this case, concentration of the unreacted DPPH free radicals) corresponds to the decrease in EPR signal (EPR-DPPH) amplitude. Therefore, the antioxidant activity of the tomato samples is expressed as a percentage,

which is calculated using the following formula:

$$\% \text{ reduction of DPPH} = \frac{A_b - A_s}{A_b} \times 100 \quad (3)$$

where the A_b is the amplitude of the blank sample and A_s is the amplitude of the tomato juice samples.

The concentration of antioxidants presented in tomato juice samples was calculated using calibration curve of L (+) ascorbic acid (0–100 mM/L) obtained from Gram Mol, Zagreb, Croatia. The results are expressed as ascorbic acid equivalents (AAE mM/L).

2.5. Microbiological characterization

The total count of yeasts and molds was determined according to the ISO 21,527–1:2008 method, while the total count of mesophilic bacteria was determined according to the ISO 4833–2:2013 method. The raw material was used for initial inoculation and for ten serials 1:10 dilutions in buffer peptone water (Merck, Darmstadt, Germany). From each dilution in duplicate, 0.1 mL aliquots were uniformly spread on a nutrient medium surface by L-stick, Dichloran Rose Bengal Chloramphenicol Agar (DRBC) (Difco, Chicago, IL, USA) for molds and yeasts or Plate Count Agar (PCA) (Merck, Darmstadt, Germany) for mesophilic bacteria. The inoculated DRBC agar plates were incubated for five days at 25 °C (± 1 °C), while the PCA agar plates were incubated for 72 h at 30 °C (± 1 °C) under aerobic conditions. After incubation, the grown colonies of molds, yeasts and bacteria were counted and CFU/ml were determined.

2.6. Statistical analysis

All analyses were performed with three replicates unless otherwise stated, and results are presented as mean \pm SD. A one-way analysis of variance (ANOVA) was performed to determine possible differences in the results with $p \leq 0.05$. The means of the treatments were separated using an unequal Tukey test for honestly significant differences (HSD) with $p \leq 0.05$. A Pearson correlation test was performed between all measured values. Statistical analyses were performed using Systat v.13.2.01 (Grafiti LLC, Palo Alto, US).

3. Results and discussion

3.1. Spin-trapping of residual radicals by EPR spectroscopy

EPR spin trapping of residual free radicals with CMH was successfully used to quantify the species of free radicals generated by both stand-alone and combined UV-A and US treatment in three treatment cycles. The so-called blank spectra ($P(\text{UV})=0$ mW, $A(\text{US})=0$ %), which consist only of untreated tomato samples and the CMH, showed no EPR signal (Fig. 2). As shown in Fig. 2, clear differences in the intensity of the EPR-CM signals were observed between the control sample, US-treated sample, and UV-A/US-treated sample, with signal intensity being proportional to the concentration of generated free radicals. Furthermore, the figure suggests an antagonistic interaction between US and UV-A treatments, as a higher EPR-CMH signal intensity was observed in samples treated with US alone compared to those subjected to the combined UV-A/US treatment, indicating that the addition of UV-A may influence or partially suppress radical formation induced by ultrasound.

The results shown in Fig. 3. confirm previous findings that both UV-A and US treatment alone generate free radicals, mainly in the form of reactive oxygen species (ROS) (Bhat, 2016; Carp et al., 2004; Char et al., 2010; Mehta et al., 2019; Nimse & Pal, 2015). The results of the spin-trapping experiments in our study show that the concentration of trapped radicals was significantly higher when only ultrasonic treatment was applied. Pearson's correlation analysis revealed a moderate negative correlation between UV-A treatment and CP concentration ($r =$

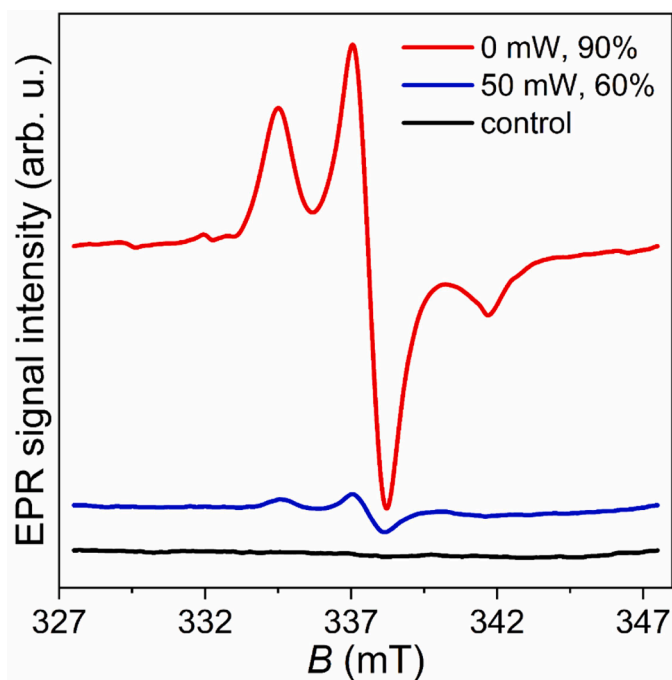
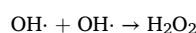
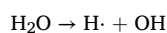


Fig. 2. The difference in EPR-CM signal intensity between US treated sample (red line), UV-A/US treated sample (blue line) and control sample (black line).

-0.5715), indicating that increasing UV-A exposure was associated with a decrease in CP concentration. In contrast, ultrasound treatment showed a moderate positive correlation with CP concentration ($r = 0.5282$), suggesting a potential enhancing effect of ultrasound on CP concentration (Figure S4, SI). In addition, the concentration of trapped radicals increased slightly but statistically significantly ($p = 0.005$) with the number of treatment cycles in all stand-alone treatments. Mechanistically, acoustic cavitation generates primary radicals inside collapsing microbubbles, creating localized extreme conditions (high temperature and pressure) that thermally decompose water into $\bullet\text{OH}$ and $\bullet\text{H}$ radicals:



During the ultrasonic treatment, the probe immersed in the reaction mixture continuously monitored the bulk temperature, which did not exceed 40 °C. It should be noted, however, that ultrasonic cavitation generates transient localized hotspots with temperatures and pressures much higher than the measured bulk values. These microenvironments are responsible for the observed enhancements in reaction rate, while the bulk temperature reflects the overall macroscopic conditions.

In the presence of UV-A, these radicals undergo accelerated recombination, including $\bullet\text{OH}$ dimerization to H_2O_2 , and are further quenched by photoexcited chromophores acting as radical traps (Koutchma, 2009; Martí et al., 2016; Vione et al., 2006; Wu et al., 2025). US-induced tissue disruption enhances this effect by releasing bound antioxidants, increasing their immediate availability for radical scavenging under UV-A exposure (Prempeh et al., 2025; Wu et al., 2025).

The results of the combined UV-A/US treatments show a significant reduction in the detected concentration of residual radicals. Moreover, the concentration remained essentially the same after the second and third cycles, suggesting that the combination of these two treatments can be used to suppress the formation of free radicals. One possible explanation is that the same process that causes the formation of free radicals under UV irradiation also enables faster recombination and neutralisation. This indicates that the formation of free radicals in the individual treatments, especially in the US treatment, which generates

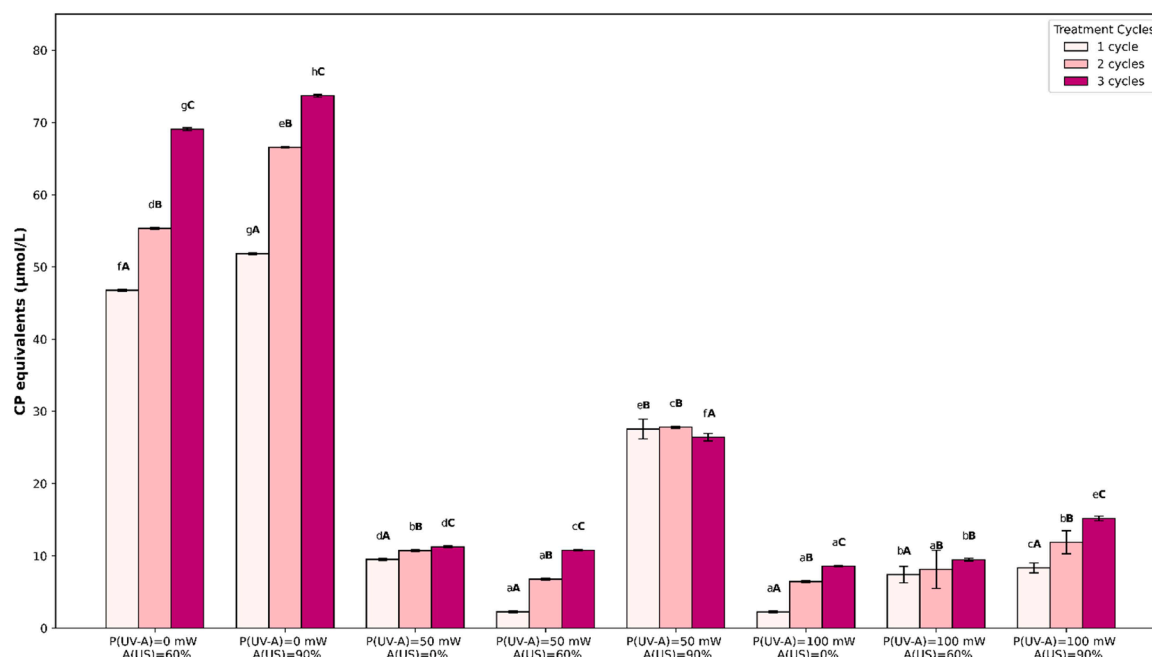


Fig. 3. Concentration of free radicals in tomato juice samples expressed as gallic acid equivalents (mg/L GAE). Different uppercase letters (A, B, C) above bars indicate statistically significant differences between cycles, while different lowercase letters (a, b, c) indicate statistically significant differences between treatments ($p \leq 0.05$, Tukey post-hoc test).

the highest concentration of free radicals, can be suppressed by the simultaneous application of a UV treatment. Under combined UV-A exposure, photochemical processes reduce the net accumulation of short-lived radicals by accelerating radical recombination and decay pathways, lowering the steady-state concentration of $\bullet\text{OH}$ despite continued ultrasonic generation (Koutchma, 2009; Vione et al., 2006). In addition, tomato juice contains a dense pool of endogenous chromophores, such as polyphenols, carotenoids, and ascorbic acid, that can be photoexcited by UV-A to reactive singlet or triplet states (Martí et al., 2016; Moreno et al., 2023). These photoexcited antioxidants act as radical sinks, reacting rapidly with US-generated radicals and effectively neutralizing oxidative intermediates before they propagate chain reactions (Moreno et al., 2023; Vione et al., 2006). US-induced tissue disruption further amplifies this effect by releasing bound phenolics and carotenoids from cellular structures, increasing their immediate availability for radical scavenging during UV-A exposure (Prempeh et al., 2025; Wu et al., 2025).

Although UV-A can photolyze H_2O_2 to regenerate $\bullet\text{OH}$ in simple aqueous systems (Vione et al., 2006), in a complex antioxidant-rich matrix such as tomato juice this effect is likely outweighed by rapid quenching via the endogenous antioxidant network, including redox cycling of ascorbate, glutathione, and phenolic compounds (Buxton et al., 1988; Niu & Liao, 2016; Prempeh et al., 2025; Vione et al., 2006; Wu et al., 2025). This creates a recombination-dominant regime in which radical decay exceeds US-induced radical generation, providing a kinetic explanation for the observed antagonistic effect (Akti & Yildiz, 2025; Vione et al., 2006). Furthermore, UV-A exposure may promote a shift in radical speciation from highly reactive ROS toward more rapidly quenched reactive nitrogen-oxygen species (RNOS), potentially explaining the reduced net radical signal under combined treatment (Gotham et al., 2020; Niu & Liao, 2016).

Furthermore, this combination can be implemented instead of the use of additives containing free radical scavengers such as garlic (Goodman et al., 2002) and other species when samples are treated with US to preserve the quality of the samples.

Hydrogen peroxide formed via radical recombination is relatively stable and contributes less strongly to EPR signals than $\bullet\text{OH}$ (Buxton

et al., 1988). In acidic tomato juice, H_2O_2 can participate in secondary reactions with nitric oxide-derived species, forming RNOS such as peroxyntirite (ONOO^-), which are rapidly consumed by phenolic compounds through nitration, effectively channeling reactive intermediates into stable, non-radical products (Buxton et al., 1988; Niu & Liao, 2016). The balance between H_2O_2 photolysis and rapid antioxidant quenching helps explain why regenerated $\bullet\text{OH}$ remains limited in tomato juice despite UV-A exposure (Buxton et al., 1988; Vione et al., 2006). This shift from ROS-dominated chemistry toward quenched RNOS pathways provides a mechanistic basis for the reduced radical signal observed under combined UV-A/US treatment (Akti & Yildiz, 2025; Vione et al., 2006). These mechanistic pathways are proposed explanations rather than experimentally confirmed processes.

Future studies employing EPR spin trapping with selective probes (e.g., DMPO for $\bullet\text{OH}$ and CPH for superoxide/peroxyntirite) are warranted to experimentally verify changes in radical speciation and to test the hypothesis that UV-A promotes a $\text{ROS} \rightarrow \text{RNOS}$ shift (Gotham, 2020).

3.2. Physicochemical characterization

3.2.1. pH, titratable acidity and total soluble solids

The type and duration of treatment had no significant effect on the pH value of the tomato samples (4.48 ± 0.08). The total soluble solids content (4.1 ± 0.4) °Brix and titratable acidity (0.24 ± 0.04) % of citric acid equivalents show similar trends when the mean values are grouped according to the type of treatment, i.e. UV-A irradiation only, ultrasound treatment only and combined UV-A and US treatment (Table 1 and Table 2). Pearson's correlation analysis revealed a weak positive correlation between UV-A treatment and TSS ($r = 0.287$) as well as TA ($r = 0.2384$). In the case of ultrasound treatment, a moderate positive correlation was observed with TSS ($r = 0.6208$), while a weak positive correlation was found with TA ($r = 0.1561$) (Figure S4, SI). The number of cycles, i.e. the duration and repetition of the cycles, did not decisively/weightily change the TSS and TA values within the same treatment type. The TSS content increased with combined UV-A and US treatment from 3.3 °Brix to a maximum of 4.6 °Brix, with the most significant increase observed with a UV-A treatment of 50 mW in

Table 1

Total soluble solids in tomato juice samples. Results (°Brix) are expressed as mean of three replicates \pm SD.

P(UV-A)/ mW	A(US)/ %	Total Soluble Solids (°Brix)		
		No. of treatment cycles		
		1	2	3
0	0		3.33 \pm 0.06	
0	60	4.00 \pm 0.00 ^{CB}	3.97 \pm 0.06 ^{CA}	3.90 \pm 0.00 ^{CA}
0	90	3.93 \pm 0.6a ^{CA}	3.97 \pm 0.06 ^{CA}	3.97 \pm 0.06 ^{cdA}
50	0	3.33 \pm 0.06 ^{AA}	3.60 \pm 0.00 ^{BB}	4.63 \pm 0.06 ^{FC}
50	60	4.63 \pm 0.06 ^{DB}	4.33 \pm 0.12 ^{DA}	4.60 \pm 0.00 ^{FB}
50	90	4.53 \pm 0.12 ^{DA}	4.57 \pm 0.06 ^{EA}	4.57 \pm 0.06 ^{EA}
100	0	3.67 \pm 0.06 ^{BA}	3.60 \pm 0.00 ^{BA}	3.60 \pm 0.00 ^{BA}
100	60	4.53 \pm 0.06 ^{DA}	4.50 \pm 0.00 ^{EA}	4.43 \pm 0.12 ^{EA}
100	90	4.03 \pm 0.03 ^{CA}	4.10 \pm 0.00 ^{CA}	4.07 \pm 0.06 ^{DA}

*Within each row, different uppercase letters (A, B, C) indicate statistically significant differences between cycles and within each column, different lowercase letters (a, b, c) indicate statistically significant differences between treatments ($p \leq 0.05$, Tukey post-hoc test).

Table 2

Titrateable acidity expressed as percentage (%) of citric acid equivalents. Measurements present as mean of three replicates \pm SD.

P(UV-A)/ mW	A(US)/ %	TA% (citric acid equivalents)		
		No. of treatment cycles		
		1	2	3
0	0		0.27 \pm 0.08	
0	60	0.18 \pm 0.01 ^{AA}	0.22 \pm 0.01 ^{AB}	0.21 \pm 0.01 ^{abcAB}
0	90	0.22 \pm 0.01a ^{abB}	0.20 \pm 0.01 ^{AA}	0.20 \pm 0.01 ^{abcAB}
50	0	0.20 \pm 0.04 ^{abA}	0.25 \pm 0.06 ^{AA}	0.28 \pm 0.03 ^{abA}
50	60	0.26 \pm 0.01 ^{abdA}	0.26 \pm 0.01 ^{AA}	0.26 \pm 0.01 ^{bcA}
50	90	0.27 \pm 0.01 ^{abA}	0.27 \pm 0.01 ^{AA}	0.29 \pm 0.01 ^{abcA}
100	0	0.20 \pm 0.01 ^{abA}	0.20 \pm 0.01 ^{AA}	0.19 \pm 0.00 ^{AA}
100	60	0.28 \pm 0.01 ^{bA}	0.28 \pm 0.00 ^{AA}	0.28 \pm 0.01 ^{bcA}
100	90	0.27 \pm 0.01 ^{abA}	0.26 \pm 0.01 ^{AA}	0.26 \pm 0.01 ^{abcA}

*Within each row, different uppercase letters (A, B, C) indicate statistically significant differences between cycles and within each column, different lowercase letters (a, b, c) indicate statistically significant differences between treatments ($p \leq 0.05$, Tukey post-hoc test).

combination with any applied US amplitude.

The TSS observed after US and combined UV-US treatments can be explained by the mechanical and cavitation effects of ultrasound. Acoustic cavitation generates microbubbles that collapse violently, producing localized high temperatures and pressures, which disrupt plant cell walls and membranes. This physical disruption facilitates the release of intracellular compounds, including sugars and other soluble solids, into the juice matrix (Anaya-Esparza et al., 2023; Mehta et al., 2022). UV-A irradiation alone does not significantly break down cell walls but can induce mild photochemical effects that slightly modify cellular structures. When combined with US, UV-A may influence the kinetic behavior of radicals generated during sonication, potentially enhancing extraction without causing additional degradation (Khadhraoui et al., 2021). The minimal change in TSS over successive treatment cycles suggests that the majority of soluble solids are released during the initial treatment, with diminishing returns for repeated cycles.

Titrateable acidity has the lowest values in separate UV and US treatments compared to the combined treatments. Another observation is that the standard deviation of titrateable acidity is significantly larger for no US treatment and low power UV treatment than for the samples subjected to higher intensity treatments such as US or combined UV-A and US treatment. This indicates a greater heterogeneity of the samples after low intensity treatments. This effect indicates further degradation of the tomato matrix by high intensity treatments and increased homogeneity of the sample (Anese et al., 2013).

Titrateable acidity (TA) is largely determined by the content of organic acids such as citric acid in tomato juice. The slight increase in TA following US and combined UV-A/US treatments can similarly be attributed to cell wall and membrane disruption, which facilitates the release of intracellular acids into the juice. UV-A alone had minimal impact on TA, indicating that photochemical effects are insufficient to release significant amounts of organic acids. The overall stability of TA across treatments and cycles suggests that these non-thermal processing methods preserve acid composition while slightly enhancing release, in contrast to thermal treatments that can cause acid degradation.

3.2.2. Determination of total polyphenol content (TPC)

Similar tendencies as for TSS and TA can also be observed for the determined values of TPC (Table 3). Statistical analysis showed no significant ($p = 0.554$) differences between cycles when ultrasound was applied alone. However, the p-value ($p = 0.000$) indicated a statistically significant effect of the applied US amplitude and correlation analysis revealed a moderately negative relationship between the US amplitude and the TPC value ($r = -0.6700$) (Figure S4, SI). This indicates that higher US amplitudes are moderately associated with lower TPC values. According to the results presented in Table 3, an increase in TPC with the number of cycles was observed at 60 % amplitude, whereas the opposite effect was observed at 90 % amplitude. Nevertheless, the TPC in US-treated samples was lower than in the control sample, but higher than in the UV-A/US treated samples.

Statistically significant increase ($p = 0.0235$) in TPC concentration was obtained in samples treated with UV-A. Higher concentrations of TPC were achieved at lower power (50 mW) with highest concentration of 224.71 mg/L of GAE. An increase in the number of cycles led to a decrease in TPC during UV-A treatments. However, all UV-A treated samples exhibited higher polyphenol concentration than the control sample.

The combined UV-A/US treatment resulted in a statistically significant decrease in TPC ($p = 0.0005$) with the highest decrease observed under the treatment of 90% US amplitude combined with 100 mW UV-A applied, suggesting a synergistic degradative effect. The decrease in TPC values is more difficult to interpret as it is probably due to a combination of thermal instability of the polyphenols and their reactions with ROS.

The results indicate that all treatments involving ultrasound (alone

Table 3

Concentration of total polyphenol compounds in tomato juice samples expressed as mg/L of gallic acid equivalents. Results are expressed as mean of three replicates \pm SD.

P(UV-A)/ mW	A(US)/ %	Total phenolic content (mg/L GAE)		
		No. of treatment cycles		
		1	2	3
0	0		147.89 \pm 28.07	
0	60	127.63 \pm 21.90 ^{aA}	133.04 \pm 3.97 ^{baA}	134.09 \pm 5.91 ^{aA}
0	90	142.01 \pm 18.02 ^{abA}	140.96 \pm 16.68 ^{baA}	128.67 \pm 8.97 ^{aA}
50	0	191.54 \pm 13.09 ^{bA}	150.16 \pm 11.67 ^{baB}	224.71 \pm 33.43 ^{bB}
50	60	135.75 \pm 8.13 ^{AB}	91.16 \pm 22.94 ^{aA}	124.92 \pm 3.15 ^{aB}
50	90	127.00 \pm 3.75 ^{aA}	120.33 \pm 5.32 ^{baA}	124.50 \pm 4.38 ^{aA}
100	0	160.31 \pm 34.63 ^{abA}	159.27 \pm 41.59 ^{bA}	139.52 \pm 12.08 ^{aA}
100	60	115.96 \pm 10.78 ^{aA}	119.08 \pm 14.07 ^{baA}	119.08 \pm 13.73 ^{aA}
100	90	113.25 \pm 3.80 ^{aA}	104.91 \pm 3.97 ^{baAB}	120.33 \pm 2.89 ^{aB}

*Within each row, different uppercase letters (A, B, C) indicate statistically significant differences between cycles and within each column, different lowercase letters (a, b, c) indicate statistically significant differences between treatments ($p \leq 0.05$, Tukey post-hoc test).

or in combination with UV-A) lead to a significant decrease in polyphenolic content, highlighting the need to optimize treatment parameters, particularly by reducing ultrasound amplitude. This effect can be attributed to the increased cavitation intensity, which, while promoting the release of compounds, may cause degradation of phenolic compounds at high amplitudes. In contrast, UV-A treatments result in an increase in phenolic content, particularly at lower power (50 mW), indicating enhanced release of phenolic compounds from tomatoes. These findings are consistent with previous reports, including (Dyshlyuk et al., 2020) and (Alabdali et al., 2020) which showed increases in total phenolic content in tomatoes ranging from 13 to 55 % depending on the UV-A wavelength. Phenolic compounds play a crucial role in photoprotection by absorbing UV-A radiation and by acting as antioxidants that reduce oxidative stress. The increase in total polyphenol content during UV-A treatment can be explained by the inactivation of polyphenol oxidase (Bi et al., 2015; Müller et al., 2014). Also, UV exposure stimulates metabolic pathways involved in their biosynthesis, leading to increased accumulation and changes in the polyphenolic profile of tomatoes. However, an increase in the number of UV-A cycles may lead to partial degradation of phenolics or a reduction in the release effect, emphasizing the importance of a balanced treatment design to enhance bioactive compound content without inducing their degradation (Mariz-Ponte et al., 2019).

Overall, the results demonstrate that treatment intensity plays a key role in balancing radical suppression and bioactive compound retention. Ultrasound treatment, particularly at higher amplitudes, generally reduced total phenolic content, indicating that strong cavitation promotes degradation rather than preservation of phenolics. In contrast, UV-A treatment increased polyphenol concentration, especially at lower irradiation power (50 mW), while excessive exposure diminished this beneficial effect. The combined UV-A/US treatment resulted in the greatest TPC reduction, suggesting a synergistic degradative action. Therefore, moderate UV-A treatment (50 mW) without high-amplitude ultrasound, or combinations employing reduced ultrasound intensity and limited cycles, appear to provide the most favourable compromise between oxidative stabilization and preservation of bioactive compounds.

3.3. Carotenoids: lycopene and beta-carotene

The total carotenoid content, expressed as the content of lycopene and beta-carotene as the predominant carotenoids, is shown in Table 4 and Table 5. The effect of US on lycopene isolation was manifested as a decrease in lycopene concentration compared to the control sample. Pearson's correlation analysis showed no meaningful correlation between UV-A treatment and lycopene content ($r = 0.0035$), while ultrasound treatment exhibited a weak positive correlation with lycopene content ($r = 0.1661$) (Figure S4, SI). A comparison of treatments performed at amplitudes of 60 % and 90 % showed a statistically significant decrease in concentration with increasing amplitude and number of cycles ($p = 0.0000$), indicating that higher amplitudes and a greater number of cycles lead to higher reduction in lycopene concentration. In contrast, an increase in lycopene concentration was observed in samples treated with UV radiation without US at a power of 100 mW, as well as a further increase with an increasing number of cycles at the same power ($p = 0.0319$). The highest concentration of lycopene, 1.287 $\mu\text{g}/\text{mL}$ was obtained in the third cycle under the power of 100 mW. The lowest lycopene concentrations were obtained at a UV power of 50 mW, where a decrease was observed compared to the treatment at 100 mW. However, in same treatment conditions, an increasing trend with respect to the number of cycles was present. In combined UV and US treatments at lower power and amplitude (50 mW and 60 % of amplitude), a decrease in lycopene concentration was observed, whereas an increase was associated with a higher number of cycles. In contrast, for treatments performed at 100 mW and amplitudes of 60 % and 90 %, lycopene concentration increased with the number of cycles, while decreasing

Table 4

Lycopene concentration ($\mu\text{g}/\text{mL}$) in tomato juice samples. Results are expressed as mean of three replicates \pm SD.

P(UV-A)/mW	A (US)/%	Lycopene ($\mu\text{g}/\text{mL}$)		
		No. of treatment cycles		
		1	2	3
0	0		0.096 \pm 0.001	
0	60	0.730 \pm 0.000 _{bcA}	0.848 \pm 0.004 _{abB}	0.822 \pm 0.005 _{abA}
0	90	0.997 \pm 0.000 ^{cA}	0.899 \pm 0.001 _{abA}	0.859 \pm 0.008 ^{ba}
50	0	0.638 \pm 0.008 _{baA}	0.731 \pm 0.008 ^{aA}	0.794 \pm 0.005 _{abA}
50	60	0.872 \pm 0.002 _{bcA}	0.885 \pm 0.002 _{abA}	1.272 \pm 0.002 ^{cB}
50	90	0.865 \pm 0.007 _{bcA}	0.913 \pm 0.002 _{abA}	0.458 \pm 0.014 ^{aA}
100	0	0.995 \pm 0.018 ^{cA}	1.061 \pm 0.106 ^{ba}	1.287 \pm 0.018 ^{cA}
100	60	0.390 \pm 0.005 _{bcA}	1.050 \pm 0.005 ^{bB}	1.022 \pm 0.004 _{bcB}
100	90	0.787 \pm 0.002 ^{aA}	0.778 \pm 0.078 ^{aA}	0.822 \pm 0.011 _{abA}

*Within each row, different uppercase letters (A, B, C) indicate statistically significant differences between cycles and within each column, different lowercase letters (a, b, c) indicate statistically significant differences between treatments ($p \leq 0.05$, Tukey post-hoc test).

Table 5

Beta-carotene concentration ($\mu\text{g}/\text{mL}$) in tomato juice samples. Results are expressed as mean of three replicates \pm SD.

P(UV-A)/mW	A (US)/%	beta-carotene ($\mu\text{g}/\text{mL}$)		
		No. of treatment cycles		
		1	2	3
0	0		0.218 \pm 0.002	
0	60	0.200 \pm 0.002 ^{aA}	0.206 \pm 0.001 _{abA}	0.208 \pm 0.004 ^{aA}
0	90	0.124 \pm 0.002 ^{aA}	0.064 \pm 0.001 _{abA}	0.146 \pm 0.012 ^{aA}
50	0	0.133 \pm 0.004 ^{aA}	0.164 \pm 0.004 _{abA}	0.191 \pm 0.001 ^{aA}
50	60	0.259 \pm 0.011 ^{aA}	0.240 \pm 0.011 ^{ba}	0.212 \pm 0.004 ^{aA}
50	90	0.166 \pm 0.004 ^{aA}	0.183 \pm 0.001 _{abA}	0.211 \pm 0.001 ^{aA}
100	0	0.274 \pm 0.009 ^{aA}	0.286 \pm 0.006 _{abA}	0.282 \pm 0.001 ^{aA}
100	60	0.151 \pm 0.006 ^{aA}	0.191 \pm 0.000 _{abA}	0.174 \pm 0.004 ^{aA}
100	90	0.141 \pm 0.004 ^{aA}	0.121 \pm 0.002 _{abA}	0.124 \pm 0.003 ^{aA}

*Within each row, different uppercase letters (A, B, C) indicate statistically significant differences between cycles and within each column, different lowercase letters (a, b, c) indicate statistically significant differences between treatments ($p \leq 0.05$, Tukey post-hoc test).

with increasing amplitude. The increase in lycopene concentration observed under prolonged UV-A treatments at an intensity of 100 mW is consistent with the findings of Dyshlyuk et al. (2020), who reported a 24–56 % increase in lycopene concentration under prolonged exposure conditions. The increase in lycopene concentration under prolonged UV-A irradiation may be related to a stress-induced upregulation of carotenoid biosynthesis, as UV treatments have been reported to alter carotenoid profiles in exposed tissues (Badmus, Ac et al., 2022). However, US appears to affect lycopene content mainly through mechanical and indirect oxidative effects on tissue structure, which can lead to compound degradation at higher amplitudes and longer exposure (Fallah et al., 2025). When combined, the balance between UV-induced biosynthetic stimulation and ultrasound-induced structural disruption likely determines the net change in lycopene concentrations, with UV-dominated conditions favoring accumulation and ultrasound-dominant conditions favoring reduction.

The concentration of beta-carotene in all samples did not depend on the number of treatment cycles. Pearson's correlation analysis revealed a weak positive correlation between UV-A treatment and beta-carotene content ($r = 0.1215$), whereas ultrasound treatment exhibited a

moderate negative correlation with beta-carotene content ($r = -0.5523$) (Figure S4, SI). The effect of ultrasound was reflected in a decrease in concentration compared to the control sample, as well as a further decrease with increasing amplitude. A similar trend was observed in treatments with UV radiation alone, without ultrasound, when a lower UV power was applied, whereas an increase in concentration was recorded at a higher UV power, where the highest beta-carotene concentration of 0.286 $\mu\text{g/mL}$ was obtained. The lowest beta-carotene concentrations (121 $\mu\text{g/mL}$) were recorded in the combined UV and US treatments. The trends observed for beta-carotene were largely similar to those reported for lycopene. Prolonged UV-A exposure appeared to stimulate carotenoid biosynthesis, resulting in increased beta-carotene concentrations at higher UV power, as UV radiation has been shown to alter carotenoid contents in other plant or microalgal systems (Badmus, Crestani et al., 2022; Mutschlechner et al., 2022; Wongnsansilp et al., 2019), although responses are compound-specific and not fully consistent across studies. US treatments primarily induced mechanical and oxidative degradation, leading to reduced concentrations at higher amplitudes (Tovar-Pérez et al., 2020; Živanović et al., 2017). In combined UV-A and US treatments, beta-carotene concentrations were lowest, suggesting that US-induced degradation outweighed UV-induced stimulation. It should be noted that lycopene is the predominant carotenoid in tomato, and structural differences between lycopene and beta-carotene, particularly the acyclic versus cyclic configuration, may contribute to differences in their stability and response to UV-A and US treatments. Overall, carotenoid concentrations appear to be influenced by the balance between UV-induced biosynthetic activation and US-induced structural disruption.

Overall, carotenoid responses indicate that treatment intensity determines the balance between compound preservation and degradation. Ultrasound treatment, particularly at higher amplitudes, generally reduced lycopene and beta-carotene concentrations, suggesting that mechanical disruption and oxidative effects promote carotenoid degradation. In contrast, UV-A treatment, especially at higher irradiation power (100 mW), stimulated carotenoid accumulation, likely due to stress-induced biosynthetic responses. However, combined UV-A/US treatments resulted in the lowest carotenoid levels, indicating that ultrasound-induced degradation predominated over UV-A stimulation. Therefore, UV-A processing at 100 mW without high-amplitude ultrasound appears to provide favourable conditions for maintaining carotenoid stability while achieving technological treatment effects.

3.4. Total antioxidant activity

The results of antioxidant activity measurements showed a significant increase following US ($p = 0.073$), UV ($p = 0.005$), and combined UV-A/US treatments, depending on the number of cycles and treatment

Table 6

Antioxidant activity of tomato juice samples expressed as percentage (%) of DPPH-EPR signal intensity. Results present mean value of three replicates \pm SD.

P(UV-A)/ mW	A (US)/ %	Radical reduction (%)		
		No. of treatment cycles		
		1	2	3
0	60	17.35 \pm 1.46 ^{abB}	15.12 \pm 1.08 ^{aA}	24.34 \pm 1.31 ^{bC}
0	90	21.93 \pm 1.10 ^{cA}	23.71 \pm 1.84 ^{bB}	24.58 \pm 2.01 ^{bB}
50	0	27.92 \pm 3.46 ^{dA}	24.99 \pm 3.83 ^{bA}	27.53 \pm 0.98 ^{dA}
50	60	28.92 \pm 1.35 ^{deB}	29.77 \pm 2.23 ^{cB}	25.18 \pm 1.53 ^{bcA}
50	90	30.17 \pm 1.50 ^{deA}	29.36 \pm 1.97 ^{cA}	27.87 \pm 1.26 ^{cdA}
100	0	19.21 \pm 2.23 ^{bA}	24.36 \pm 1.07 ^{bB}	24.95 \pm 1.41 ^{bcB}
100	60	32.96 \pm 1.57 ^{fc}	31.49 \pm 1.02 ^{cB}	27.02 \pm 1.02 ^{cdA}
100	90	30.63 \pm 1.33 ^{efB}	30.75 \pm 1.50 ^{cB}	16.15 \pm 2.50 ^{aA}

*Within each row, different uppercase letters (A, B, C) indicate statistically significant differences between cycles and within each column, different lowercase letters (a, b, c) indicate statistically significant differences between treatments ($p \leq 0.05$, Tukey post-hoc test).

parameters. The highest reduction (Table 6) of the EPR-DPPH signal was observed under combined UV-A/US treatments (31.49 %), whereas the lowest was recorded in the US treated sample in two cycles (15.12 %). The effects of treatments on antioxidant concentration followed the same trend as the percentage reduction of the EPR-DPPH signal (Table S2, SI). The effects of UV-A and US treatments on bioactive compounds and antioxidant activity exhibited distinct and independent patterns. TPC reached its maximum of 224.71 mg/L GAE under UV-A at 50 mW in the third treatment cycle, while lycopene reached maximum concentration of 1.287 $\mu\text{g/mL}$ under UV-A at 100 mW in the third cycle, and beta-carotene showed its highest concentration of 0.286 $\mu\text{g/mL}$ under UV-A at 100 mW in the second cycle. Pearson's correlation analysis (Figure S4, SI) showed that antioxidant activity had a weak positive correlation with lycopene ($r = 0.2312$) and a weak negative correlation with beta-carotene ($r = -0.1762$) and TPC ($r = -0.2224$), suggesting that other naturally occurring antioxidants in tomato pulp, including ascorbic acid, may contribute to the overall antioxidant activity. Despite variations in individual compounds, antioxidant activity remained elevated in many treatments, indicating that it reflects the combined contribution of all bioactive compounds rather than a single component. This suggests that antioxidant activity cannot be attributed to any individual compound but represents a complex response of all bioactive components in tomato pulp, collectively influenced by UV, US, and combined UV-A/US treatments. The observed enhancement of antioxidant activity is consistent with previous studies demonstrating that UV and US treatments can increase the antioxidant activity of treated samples relative to untreated controls. Overall, these results highlight the synergistic effects of UV-induced biosynthetic stimulation and US-facilitated compound release, and confirm that TPC, lycopene, beta-carotene, and antioxidant activity each follow their own distinct trends, with the overall antioxidant potential arising from the combined contributions of all components rather than from any single bioactive compound. Moreover, previous studies have shown that both UV and US treatments individually can enhance the concentration of bioactive compounds and antioxidant activity (Dyshlyuk et al., 2020; Lu et al., 2020; Mariz-Ponte et al., 2019; Mditswha et al., 2017; Tovar-Pérez et al., 2020), while, to our knowledge, no studies have yet investigated the combined effect of UV/US treatments. Accordingly, the results of the present study are consistent with these findings, as antioxidant activity was increased in all treated samples, with the greatest enhancement observed under the combined UV-A/US treatment.

3.5. Microbiological analysis

All samples, both, the treated and the control samples, showed microbial loads (total aerobic microbial count (TAMC), total yeast count (TYC), total mold content (TMC) and total yeast and mold count (TYMC), with log values below 4 (Table 7). A significant difference in the inactivation of yeasts was observed between the treatments with UV-A irradiation in contrast to the treatments without UV-A. This finding is consistent with earlier studies by Thabet et al. and Shirai et al. who also found that UV-A light has a big impact on the inactivation of yeast, and with Adekunle et al. who used US to inactivate microorganisms in tomato juice (Adekunle et al., 2010; Shirai et al., 2022; Thabet et al., 2013). For the treatments including UV-A irradiation, the values are between 1.00 and 1.96, which is close to the values of the three cycles of the US treatments with values of 2.15 and 2.18. In some combinations of treatments and the blank sample, the TYM count was below the detection limit. The log(CFU/mL) of total aerobic microbial count (TAMC) value for the control group was 2.49, and for the treated samples it varied between 2.08 and 3.18 with an average value of 2.76 ± 0.30 . The highest TAMC values were obtained with a combined UV-A and US treatments, while the lowest value was obtained with an US treatment alone.

It is well established that the effectiveness of UV-A irradiation in water treatment is significantly limited by several factors, including

Table 7

Microbiological analysis of treated samples, expressed as log(CFU/mL). Values are shown for total aerobic microbial count (TAMC), total yeast count (TYC), total mold content (TMC), and total yeast and mold count (TYMC).

P(UV-A)/ mW	A(US)/%	TAMC (log(CFU/mL))			TYC (log(CFU/mL))			TMC (log(CFU/mL))			TYMC (log(CFU/mL))		
		No. of treatment cycles			No. of treatment cycles			No. of treatment cycles			No. of treatment cycles		
		1	2	3	1	2	3	1	2	3	1	2	3
0	0		2.49			n.d.			n.d.			n.d.	
0	60	2.41	2.26	2.40	2.68	2.54	2.08	n.d.	n.d.	1.48	2.68	2.54	2.18
0	90	2.48	2.57	2.46	2.73	2.61	2.11	n.d.	1.65	1.00	2.73	2.66	2.15
50	0	3.18	2.08	2.77	1.00	1.30	1.30	n.d.	n.d.	n.d.	1.00	1.30	1.30
50	60	3.00	2.92	2.65	1.48	1.30	n.d.	n.d.	1.00	n.d.	1.48	1.48	n.d.
50	90	2.92	3.00	2.65	1.00	1.48	1.48	1.00	n.d.	n.d.	1.30	1.48	1.48
100	0	2.83	2.74	2.72	1.00	1.32	1.48	n.d.	n.d.	n.d.	1.00	1.32	1.48
100	60	3.08	3.18	3.15	1.65	1.96	1.48	n.d.	n.d.	1.30	1.65	1.96	1.70
100	90	3.08	2.93	2.75	1.56	n.d.	n.d.	n.d.	n.d.	n.d.	1.56	n.d.	n.d.

*n.d. - not detected.

reduced light penetration in turbid media, particle shielding (shadowing effects), and the complex relationship between applied dose and absorption characteristics (González et al., 2023). Consequently, the full potential of UV-A is expected to be lower in complex matrices such as tomato juice.

However, the results presented in Table 7 indicate that there was no significant reduction in TMC or TYMC. This is likely due to the mild treatment with US, UV-A light, and their combination. As shown in Table 7, the highest reduction in TAMC was observed in the treatment with two cycles of UV-A alone at a power of 50 mW, with a reduction of 190 CFU/mL, and in the US treatment alone at an amplitude of 60 % after two cycles, where a reduction of 130 CFU/mL was achieved. For yeasts and moulds, an increase in the cell count was observed in almost all samples, although the count remained below 550 CFU/mL (Table 7).

In the present study, the initial microbial load was relatively low (~2.5 log CFU/mL), and the observed microbial reduction was therefore limited. To better demonstrate the antimicrobial potential of UV-A in such matrices, future studies should employ higher initial microbial concentrations, where treatment effects would be more pronounced. Nevertheless, even with the relatively small difference between microbial counts before and after treatment, UV-A irradiation demonstrated potential for microbial reduction in this type of matrix.

4. Conclusion

This study demonstrates that UV-A, US, and combined UV-A/US treatments significantly influence concentration of bioactive compounds, antioxidant activity, and free radical generation in tomato pulp. From a microbiological perspective, all treated and control samples exhibited low microbial loads, with total aerobic bacteria, yeasts, and moulds remaining below 4 log CFU/mL. UV-A irradiation showed a more pronounced effect on yeast inactivation compared to treatments without UV-A, while ultrasound treatments produced comparable reductions in total aerobic microbial counts. No significant reductions in mold or total yeast and mold counts were observed, likely due to the mild nature of the applied treatments and the complexity of the tomato matrix. Combined UV-A/US treatments effectively enhanced antioxidant activity in tomato pulp, with the highest DPPH reduction observed under combined treatment (31.49 %) and the greatest CP value recorded under ultrasound at 90 % amplitude after three cycles (73.72 μmol/L). EPR analysis using the CMH spin trapping method showed that ultrasound had the strongest effect on free radical generation, while UV-A alone induced lower CP equivalents and combined UV-A/US treatments resulted in intermediate values, indicating a non-additive interaction. In contrast, UV-A treatments alone were more effective in increasing concentrations of bioactive compounds, reaching maximum values of 224.71 mg/L GAE for total polyphenols, 1.287 μg/mL for lycopene, and 0.286 μg/mL for beta-carotene. The observed effects may be explained

by ultrasound-induced ROS generation, as indicated by the higher CP values at increasing US amplitude, while UV-A alone seems to activate endogenous antioxidant pathways, reducing radical accumulation. The intermediate CP values observed in combined UV-A/US treatments suggest a modulatory effect of UV-A on US-induced radicals, consistent with a non-additive interaction. These trends indicate a potential shift in the ROS/RNS balance and possible antioxidant photoactivation under UV-A exposure. These findings suggest that while combination treatments are promising for enhancing antioxidant activity, further optimization of UV-A and US parameters is necessary to simultaneously maximize both antioxidant activity and bioactive compound content.

To our knowledge, this is the first study to investigate the combined effect of UV-A and US on tomato pulp, highlighting its potential for improving the nutritional and functional quality of tomato-based products and guiding future research on treatment optimisation and mechanistic understanding. Nevertheless, several limitations of the present study should be acknowledged. The investigation focused on short-term effects, and storage stability of treated tomato pulp was not evaluated, which should be considered in future studies. In addition, although UV-A was selected due to its potentially milder impact on quality parameters, other UV ranges, such as UV-C, may provide stronger antimicrobial effects and require further comparative evaluation. Future research should also include sensory analysis to assess consumer acceptability and scale-up trials to confirm industrial feasibility. Moreover, further optimisation of processing parameters could be achieved using response surface methodology, enabling simultaneous evaluation of key factors such as ultrasound amplitude, number of treatment cycles, and UV exposure conditions.

Ethical statement

The authors state that the research presented does not include animal or human studies.

CRediT authorship contribution statement

Kristina Smokrović: Writing – review & editing, Writing – original draft, Visualization, Validation, Methodology, Investigation, Formal analysis, Data curation, Conceptualization. **Sanda Pleslić:** Writing – review & editing, Writing – original draft, Visualization, Validation, Methodology, Investigation, Formal analysis, Data curation, Conceptualization. **Franka Markić:** Writing – review & editing, Writing – original draft, Validation, Methodology, Investigation, Formal analysis, Data curation. **Senada Muratović:** Writing – review & editing, Writing – original draft, Validation, Methodology, Investigation, Formal analysis, Data curation. **Tomislava Vukušić Pavičić:** Writing – review & editing, Writing – original draft, Validation, Supervision, Methodology, Investigation, Conceptualization. **Višnja Stulić:** Writing – review & editing,

Writing – original draft, Validation, Methodology, Investigation, Formal analysis, Data curation. **Manuela Zadavec:** Writing – review & editing, Writing – original draft, Validation, Methodology, Investigation, Formal analysis, Data curation. **Nadica Maltar-Strmečki:** Writing – review & editing, Writing – original draft, Visualization, Validation, Supervision, Resources, Project administration, Methodology, Investigation, Funding acquisition, Conceptualization.

Declaration of competing interest

The authors declare that they have no known competing financial interests or personal relationships that could have appeared to influence the work reported in this paper.

Acknowledgments

This study was funded by the European Union's Horizon 2020-PRIMA Section I Program under grant agreement #2032 (FunTomp).

Supplementary materials

Supplementary material associated with this article can be found, in the online version, at [doi:10.1016/j.afres.2026.101988](https://doi.org/10.1016/j.afres.2026.101988).

Data availability

The datasets generated during the current study are available from the corresponding authors.

References

- Adekunte, A. O., Tiwari, B. K., Cullen, P. J., Scannell, A. G. M., & O'Donnell, C. P. (2010). Effect of sonication on colour, ascorbic acid and yeast inactivation in tomato juice. *Food Chemistry*, 122(3), 500–507. <https://doi.org/10.1016/j.foodchem.2010.01.026>
- Akti, N., & Yildiz, S. (2025). Exploring ultrasound-induced free radical formation: A comparative study in water and sour cherry juice using glutathione and terephthalic acid indicators. *Ultrasonics Sonochemistry*, 112. <https://doi.org/10.1016/j.ultsonch.2024.107193>
- Alabdali, T. A. M., Icyer, N. C., Ozkaya, G. U., & Durak, M. Z. (2020). Effect of stand-alone and combined ultraviolet and ultrasound treatments on physicochemical and microbial characteristics of pomegranate juice. *Applied Sciences-Basel*, 10(16). <https://doi.org/10.3390/app10165458>
- Ali, M. Y., Sina, A. I., Khandker, S. S., Neesa, L., Tanvir, E. M., Kabir, A., Khalil, M. I., & Gan, S. H. (2021). Nutritional composition and bioactive compounds in tomatoes and their impact on Human health and disease: A review. *Foods (Basel, Switzerland)*, 10(1). <https://doi.org/10.3390/foods10010045>. Article ARTN 45.
- Anaya-Esparza, L. M., Aurora-Vigo, E. F., Villagrán, Z., Rodríguez-Lafitte, E., Ruvalcaba-Gómez, J. M., Solano-Cornejo, M. A., Zamora-Gasga, V. M., Montalvo-González, E., Gómez-Rodríguez, H., Aceves-Aldrete, C. E., & González-Silva, N. (2023). Design of experiments for optimizing ultrasound-assisted extraction of bioactive compounds from plant-based sources. *Molecules (Basel, Switzerland)*, 28(23). <https://doi.org/10.3390/molecules28237752>
- Anbar, M., Meyerstein, D., & Neta, P. (1966). The reactivity of aromatic compounds toward hydroxyl radicals. *The Journal of Physical Chemistry*, 70(8), 2660–2662. <https://doi.org/10.1021/j100880a034>
- Anese, M., Mirolo, G., Beraldo, P., & Lippe, G. (2013). Effect of ultrasound treatments of tomato pulp on microstructure and lycopene bioaccessibility. *Food Chemistry*, 136(2), 458–463. <https://doi.org/10.1016/j.foodchem.2012.08.013>
- Ashokkumar, M. (2011). The characterization of acoustic cavitation bubbles - an overview. *Ultrasonics Sonochemistry*, 18(4), 864–872. <https://doi.org/10.1016/j.ultsonch.2010.11.016>
- Ates, E. G., Bal, M., Karasu, M. C., Cifte, N. E., Erdem, F., Gul, M. R., Tas, O., Karsli, G. T., Pleslic, S., Smokrović, K., Maltar-Strmečki, N., Abiad, M. G., Dukic, J., Jambrak, A. R., Tchoukouang, R. D., Vieira, M. C., Antunes, M. D., Mert, B., Sumnu, G., ... Oztop, M. (2025). Reformulation and characterization of mediterranean ingredients by novel technologies. *Food Engineering Reviews*. <https://doi.org/10.1007/s12393-025-09401-0>
- Badmus, U. O., Ac, A., Klem, K., Urban, O., & Jansen, M. A. K. (2022). A meta-analysis of the effects of UV radiation on the plant carotenoid pool. *Plant Physiology and Biochemistry*, 183, 36–45. <https://doi.org/10.1016/j.plaphy.2022.05.001>
- Badmus, U. O., Crestani, G., Cunningham, N., Havaux, M., Urban, O., & Jansen, M. A. K. (2022). UV radiation induces specific changes in the carotenoid profile of *Arabidopsis thaliana*. *Biomolecules*, 12(12). <https://doi.org/10.3390/biom12121879>
- Bagryanskaya, E. G., Krumkacheva, O. A., Fedin, M. V., & Marque, S. R. A. (2015). Chapter fourteen - development and application of spin traps, spin probes, and spin labels. In P. Z. Qin, & K. Warncke (Eds.), *Methods in enzymology*: 563. *Methods in enzymology* (pp. 365–396). London, UK: Academic Press. <https://doi.org/10.1016/bs.mie.2015.06.004>
- Bal, M., Ates, E. G., Erdem, F., Karsli, G. T., Karasu, M. C., Ozarda, O., Mert, B., & Oztop, M. H. (2024). Rheological and sensorial behavior of tomato product enriched with pea protein and olive powder. *Frontiers in Sustainable Food Systems*, 8. <https://doi.org/10.3389/fsufs.2024.1358520>. Article ARTN 1358520.
- Barbosa-Cánovas, G. V., Donsì, F., Yildiz, S., Candogan, K., Pokhrel, P. R., & Guadarrama-Lezama, A. Y. (2022). Nonthermal processing technologies for stabilization and enhancement of bioactive compounds in foods. *Food Engineering Reviews*, 14(1), 63–99. <https://doi.org/10.1007/s12393-021-09295-8>
- Basdemir, E., Ince, A. E., Kizgin, S., Ozel, B., Ozarda, O., Sumnu, S. G., & Oztop, M. H. (2024). Physicochemical and sensorial properties of tomato leathers at different drying conditions. *Journal of Food Science*, 89(5), 2659–2671. <https://doi.org/10.1111/1750-3841.17061>
- Bhat, R. (2016). Impact of ultraviolet radiation treatments on the quality of freshly prepared tomato (*Solanum lycopersicum*) juice. *Food Chemistry*, 213, 635–640. <https://doi.org/10.1016/j.foodchem.2016.06.096>
- Bi, X. F., Hemar, Y., Balaban, M. O., & Liao, X. J. (2015). The effect of ultrasound on particle size, color, viscosity and polyphenol oxidase activity of diluted avocado puree. *Ultrasonics Sonochemistry*, 27, 567–575. <https://doi.org/10.1016/j.ultsonch.2015.04.011>
- Brand-Williams, W., Cuvelier, M. E., & Berset, C. (1995). Use of a free-radical method to evaluate antioxidant activity. *Food Science and Technology-Lebensmittel-Wissenschaft & Technologie*, 28(1), 25–30. <Go to ISI>://WOS:A1995QH21700005.
- Buxton, G. V., Greenstock, C. L., Helman, W. P., & Ross, A. B. (1988). Critical-review of rate constants for reactions of hydrated electrons, hydrogen-atoms and hydroxyl radicals (.Oh/.O-) in aqueous-solution. *Journal of Physical and Chemical Reference Data*, 17(2), 513–886. <https://doi.org/10.1063/1.555805>
- Carp, O., Huisman, C. L., & Reller, A. (2004). Photoinduced reactivity of titanium dioxide. *Progress in Solid State Chemistry*, 32(1–2), 33–177. <https://doi.org/10.1016/j.progsolidchem.2004.08.001>
- Char, C. D., Mitilnaki, E., Guerrero, S. N., & Alzamora, S. M. (2010). Use of high-intensity ultrasound and UV-C light to inactivate some microorganisms in fruit juices. *Food and Bioprocess Technology*, 3(6), 797–803. <https://doi.org/10.1007/s11947-009-0307-7>
- Cheng, J. H., Lv, X. Y., Pan, Y. Y., & Sun, D. W. (2020). Foodborne bacterial stress responses to exogenous reactive oxygen species (ROS) induced by cold plasma treatments. *Trends in Food Science & Technology*, 103, 239–247. <https://doi.org/10.1016/j.tifs.2020.07.022>
- Colle, I. J. P., Lemmens, L., Van Buggenhout, S., Van Loey, A. M., & Hendrickx, M. E. (2013). Modeling lycopene degradation and isomerization in the presence of lipids. *Food and Bioprocess Technology*, 6(4), 909–918. <https://doi.org/10.1007/s11947-011-0714-4>
- Cui, B. Z., Sun, Y. A., Wang, K., Liu, Y., Fu, H. F., Wang, Y. Q., & Wang, Y. Y. (2022). Pasteurization mechanism on the cellular level of radio frequency heating and its possible non-thermal effect. *Innovative Food Science & Emerging Technologies*, 78. <https://doi.org/10.1016/j.ifset.2022.103026>. Article ARTN 103026.
- Dikalov, S. I., Kirilyuk, I. A., Voinov, M., & Grigor'ev, I. A. (2011). EPR detection of cellular and mitochondrial superoxide using cyclic hydroxylamines. *Free Radical Research*, 45(4), 417–430. <https://doi.org/10.3109/10715762.2010.540242>
- Dyshlyuk, L., Babich, O., Prosekov, A., Ivanova, S., Pavsky, V., & Chaplygina, T. (2020). The effect of postharvest ultraviolet irradiation on the content of antioxidant compounds and the activity of antioxidant enzymes in tomato. *Heliyon*, 6(1). <https://doi.org/10.1016/j.heliyon.2020.e03288>
- Fallah, A. S., Touranlou, F. A., & Rezaie, M. (2025). Ultrasound technology and tomato industry: A review. *Ultrasonics Sonochemistry*, 118. <https://doi.org/10.1016/j.ultsonch.2025.107374>
- Giulitti, S., Cinquemani, C., & Spilimbergo, S. (2011). High pressure gases: Role of dynamic intracellular pH in pasteurization. *Biotechnology and Bioengineering*, 108(5), 1211–1214. <https://doi.org/10.1002/bit.21019>
- González, Y., Gómez, G., Moeller-Chávez, G. E., & Vidal, G. (2023). UV disinfection systems for wastewater treatment: Emphasis on reactivation of microorganisms. *Sustainability*, 15(14). <https://doi.org/10.3390/su15141262>
- Goodman, B. A., Glidewell, S. M., Arbuckle, C. M., Bernardin, S., Cook, T. R., & Hillman, J. R. (2002). An EPR study of free radical generation during maceration of uncooked vegetables. *Journal of the Science of Food and Agriculture*, 82(10), 1208–1215. <https://doi.org/10.1002/jsfa.1180>
- Gotham, J. P., Li, R., Tipple, T. E., Lancaster, J. R., Liu, T., & Li, Q. (2020). Quantitation of spin probe-detectable oxidants in cells using electron paramagnetic resonance spectroscopy: To probe or to trap? *Free Radical Biology and Medicine*, 154, 84–94. <https://doi.org/10.1016/j.freeradbiomed.2020.04.020>
- Guasch-Ferré, M., & Willett, W. C. (2021). The Mediterranean diet and health: A comprehensive overview. *Journal of Internal Medicine*, 290(3), 549–566. <https://doi.org/10.1111/joim.13333>
- Jiménez-Sánchez, C., Lozano-Sánchez, J., Segura-Carretero, A., & Fernández-Gutiérrez, A. (2017a). Alternatives to conventional thermal treatments in fruit-juice processing. Part 1: Techniques and applications. *Critical Reviews in Food Science and Nutrition*, 57(3), 501–523. <https://doi.org/10.1080/10408398.2013.867828>
- Jiménez-Sánchez, C., Lozano-Sánchez, J., Segura-Carretero, A., & Fernández-Gutiérrez, A. (2017b). Alternatives to conventional thermal treatments in fruit-juice processing. Part 2: Effect on composition, phytochemical content, and physicochemical, rheological, and organoleptic properties of fruit juices. *Critical Reviews in Food Science and Nutrition*, 57(3), 637–652. <https://doi.org/10.1080/10408398.2014.914019>
- Khadhraoui, B., Ummat, V., Tiwari, B. K., Fabiano-Tixier, A. S., & Chemat, F. (2021). Review of ultrasound combinations with hybrid and innovative techniques for

- extraction and processing of food and natural products. *Ultrasonics Sonochemistry*, 76. <https://doi.org/10.1016/j.ulsonch.2021.105625>
- Khan, N., Wilmot, C. M., Rosen, G. M., Demidenko, E., Sun, J., Joseph, J., O'Hara, J., Kalyanaraman, B., & Swartz, H. M. (2003). Spin traps: In vitro toxicity and stability of radical adducts. *Free Radical Biology and Medicine*, 34(11), 1473–1481. [https://doi.org/10.1016/S0891-5849\(03\)00182-5](https://doi.org/10.1016/S0891-5849(03)00182-5)
- Kouchma, T. (2009). Advances in ultraviolet light technology for non-thermal processing of liquid foods. *Food and Bioprocess Technology*, 2(2), 138–155. <https://doi.org/10.1007/s11947-008-0178-3>
- Kupina, S., Fields, C., Roman, M. C., & Brunelle, S. L. (2018). Determination of total phenolic content using the folin-C assay: Single-laboratory validation, first action 2017.13. *Journal of Aoac International*, 101(5), 1466–1472. <https://doi.org/10.5740/jaoacint.18-0031>
- Li, R., Jia, Z., & Trush, M. A. (2016). Defining ROS in biology and medicine. *React Oxy Species (Apex)*, 1(1), 9–21. <https://doi.org/10.20455/ros.2016.803>
- Li, W., Su, Q., Chong, N., Zhang, X. L., Zhao, R., & Song, H. Y. (2023). Nondestructive evaluation of polyphenol oxidase activity in tomato based on segmentation of vis-NIR spectral graph characteristics. *Infrared Physics & Technology*, 131. <https://doi.org/10.1016/j.infrared.2023.104652>. Article ARTN 104652.
- Lopez-Sanchez, P., Nijssen, J., Blonk, H. C. G., Bialek, L., Schumm, S., & Langton, M. (2011). Effect of mechanical and thermal treatments on the microstructure and rheological properties of carrot, broccoli and tomato dispersions. *Journal of the Science of Food and Agriculture*, 91(2), 207–217. <https://doi.org/10.1002/jsfa.4168>
- Lu, C. W., Ding, J. Z., Park, H. K., & Feng, H. (2020). High intensity ultrasound as a physical elicitor affects secondary metabolites and antioxidant capacity of tomato fruits. *Food Control*, 113. <https://doi.org/10.1016/j.foodcont.2020.107176>
- Mariz-Ponte, N., Martins, S., Gonçalves, A., Correia, C. M., Ribeiro, C., Dias, M. C., & Santos, C. (2019). The potential use of the UV-A and UV-B to improve tomato quality and preference for consumers. *Scientia Horticulturae*, 246, 777–784. <https://doi.org/10.1016/j.scienta.2018.11.058>
- Martí, R., Roselló, S., & Cebolla-Cornejo, J. (2016). Tomato as a source of carotenoids and polyphenols targeted to cancer prevention. *Cancers*, 8(6). <https://doi.org/10.3390/cancers8060058>. Article 58.
- Mason, T. J., Lorimer, J. P., Bates, D. M., & Zhao, Y. (1994). Dosimetry in sonochemistry - the use of aqueous terephthalate ion as a fluorescence monitor. *Ultrasonics Sonochemistry*, 1(2), S91–S95. [https://doi.org/10.1016/1350-4177\(94\)90004-3](https://doi.org/10.1016/1350-4177(94)90004-3)
- Mditshwa, A., Magwaza, L. S., Tesfay, S. Z., & Mbili, N. C. (2017). Effect of ultraviolet irradiation on postharvest quality and composition of tomatoes: A review. *Journal of Food Science and Technology-Mysore*, 54(10), 3025–3035. <https://doi.org/10.1007/s13197-017-2802-6>
- Mehta, D., Sharma, N., Bansal, V., Sangwan, R. S., & Yadav, S. K. (2019). Impact of ultrasonication, ultraviolet and atmospheric cold plasma processing on quality parameters of tomato-based beverage in comparison with thermal processing. *Innovative Food Science & Emerging Technologies*, 52, 343–349. <https://doi.org/10.1016/j.ifset.2019.01.015>
- Mehta, N., Jayapriya, S., Kumar, P., Verma, A. K., Umaraw, P., Khatkar, S. K., Khatkar, A. B., Pathak, D., Kaka, U., & Sazili, A. Q. (2022). Ultrasound-assisted extraction and the encapsulation of bioactive components for food applications. *Foods (Basel, Switzerland)*, 11(19). <https://doi.org/10.3390/foods11192973>
- Moreno, A. G., Woolley, J. M., Domínguez, E., de Cózar, A., Heredia, A., & Stavros, V. G. (2023). Synergic photoprotection of phenolic compounds present in tomato fruit cuticle: A spectroscopic investigation in solution. *Physical Chemistry Chemical Physics*, 25(18), 12791–12799. <https://doi.org/10.1039/d3cp00630a>
- Müller, A., Noack, L., Greiner, R., Stahl, M. R., & Posten, C. (2014). Effect of UV-C and UV-B treatment on polyphenol oxidase activity and shelf life of apple and grape juices. *Innovative Food Science & Emerging Technologies*, 26, 498–504. <https://doi.org/10.1016/j.ifset.2014.05.014>
- Mutschlechner, M., Walter, A., Colleselli, L., Griesbeck, C., & Schöbel, H. (2022). Enhancing carotenogenesis in terrestrial microalgae by UV-A light stress. *Journal of Applied Phycology*, 34(4), 1943–1955. <https://doi.org/10.1007/s10811-022-02772-5>
- Nagata, M., & Yamashita, I. (1992). Simple method for simultaneous determination of chlorophyll and carotenoids in tomato fruit. *Journal of the Japanese Society for Food Science and Technology-Nippon Shokuhin Kagaku Kogaku Kaishi*, 39(10), 925–928. <Go to ISI>://WOS:A1992JX29900014.
- Nimse, S. B., & Pal, D. (2015). Free radicals, natural antioxidants, and their reaction mechanisms. *Rsc Advances*, 5(35), 27986–28006. <https://doi.org/10.1039/c4ra13315c>
- Niu, L. J., & Liao, W. B. (2016). Hydrogen peroxide signaling in plant development and abiotic responses: Crosstalk with nitric oxide and calcium. *Frontiers in Plant Science*, 7. <https://doi.org/10.3389/fpls.2016.00230>. Article 230.
- Noorisefat, F., Nateghi, L., Kaviani, F., Rashidi, L., & Khosravi-Darani, K. (2025). Investigation of nutritional and microbial properties of ultrasound pretreated sour cherry juice. *Applied Food Research*, 5(1). <https://doi.org/10.1016/j.afres.2024.100638>
- Petrier, C., Jeunet, A., Luche, J. L., & Reverdy, G. (1992). Unexpected frequency-effects on the rate of oxidative processes induced by ultrasound. *Journal of the American Chemical Society*, 114(8), 3148–3150. <https://doi.org/10.1021/ja00034a077>
- Premph, N. Y. A., Nunekpeku, X., Murugesan, A., & Li, H. H. (2025). Ultrasound in the food industry: Mechanisms and applications for non-invasive texture and quality analysis. *Foods (Basel, Switzerland)*, 14(12). <https://doi.org/10.3390/foods14122057>
- Rubio, C. P., & Cerón, J. J. (2021). Spectrophotometric assays for evaluation of reactive oxygen species (ROS) in serum: General concepts and applications in dogs and humans. *Bmc Veterinary Research*, 17(1). <https://doi.org/10.1186/s12917-021-02924-8>. Article ARTN 226.
- Shirai, A., Kunimi, H., & Tsuchiya, K. (2022). Antifungal action of the combination of ferulic acid and ultraviolet-A irradiation against. *Journal of Applied Microbiology*, 132(4), 2957–2967. <https://doi.org/10.1111/jam.15407>
- Sies, H., Berndt, C., & Jones, D. P. (2017). Oxidative stress. *Annual Review of Biochemistry*, 86, 715–748. <https://doi.org/10.1146/annurev-biochem-061516-045037> (Volume 86, 2017).
- Spagna, G., Barbagallo, R. N., Chisari, M., & Branca, F. (2005). Characterization of a tomato polyphenol oxidase and its role in browning and lycopene content. *Journal of Agricultural and Food Chemistry*, 53(6), 2032–2038. <https://doi.org/10.1021/jf040336i>
- Thabet, S., Weiss-Gayet, M., Dapozze, F., Cotton, P., & Guillard, C. (2013). Photocatalysis on yeast cells: Toward targets and mechanisms. *Applied Catalysis B-Environmental*, 140, 169–178. <https://doi.org/10.1016/j.apcatb.2013.03.037>
- Tovar-Pérez, E. G., Aguilera-Aguirre, S., López-García, U., Valdez-Morales, M., Ibarra-Zurita, A. K., Ortiz-Basurto, R. I., & Chacón-López, A. (2020). Effect of ultrasound treatment on the quality and contents of polyphenols, lycopene and rutin in tomato fruits. *Czech Journal of Food Sciences*, 38(1), 20–27. <https://doi.org/10.17221/189/2019-Cjfs>
- Trinh, Q. T., Golio, N., Cheng, Y., Cha, H., Tai, K. U., Ouyang, L., Zhao, J., Tran, T. S., Nguyen, T.-K., Zhang, J., An, H., Wei, Z., Jerome, F., Amaniampong, P. N., & Nguyen, N.-T. (2025). Sonochemistry and sonocatalysis: Current progress, existing limitations, and future opportunities in green and sustainable chemistry [10.1039/D5GC01098E]. *Green Chemistry*, 27(18), 4926–4958. <https://doi.org/10.1039/D5GC01098E>
- Vione, D., Maurino, V., Minero, C., Pelizzetti, E., Harrison, M. A. J., Olariu, R. I., & Arsene, C. (2006). Photochemical reactions in the tropospheric aqueous phase and on particulate matter. *Chemical Society Reviews*, 35(5), 441–453. <https://doi.org/10.1039/B510796M>
- Wongsansilp, T., Yokthongwattana, K., Roytrakul, S., & Juntawong, N. (2019). β -carotene production of UV-C induced under salt stress. *Journal of Pure and Applied Microbiology*, 13(1), 193–200. <https://doi.org/10.22207/jpam.13.1.20>
- Wu, X. G., Shen, T. T., Liu, X. Y., Zhang, G. M., Qian, X. Q., & Yang, W. L. (2025). Unveiling the mechanisms of ultrasonic radiation-induced free radical stress on algal communities: Insights into growth inhibition, photosynthetic disruption, and antioxidant defense responses. *Ultrasonics Sonochemistry*, 115. <https://doi.org/10.1016/j.ulsonch.2025.107297>
- Yanagida, H., Masubuchi, Y., Minagawa, K., Ogata, T., Takimoto, J., & Koyama, K. (1999). A reaction kinetics model of water sonolysis in the presence of a spin-trap. *Ultrasonics Sonochemistry*, 5(4), 133–139. [https://doi.org/10.1016/S1350-4177\(98\)00020-0](https://doi.org/10.1016/S1350-4177(98)00020-0)
- Yikmis, S., Ates, A., Demirel, S., Levent, O., Tokatli, N., Demirok, N. T., Aljabbair, M. O., Karrar, E., Althawab, S. A., & Ahmed, I. A. M. (2025). Thermo-sonication-enhanced bioaccessibility and functional quality of dill juice: An digestion approach. *Frontiers in Nutrition*, 12. <https://doi.org/10.3389/fnut.2025.1666391>
- Zawawi, N. A. F., Hazmi, N. A. M., How, M. S., Kantono, K., Silva, F. V. M., & Sulaiman, A. (2022). Thermal, high pressure, and ultrasound inactivation of various fruit cultivars' Polyphenol oxidase: Kinetic inactivation models and estimation of treatment energy requirement. *Applied Sciences-Basel*, 12(4), Article 1864. <https://doi.org/10.3390/app12041864>. Article ARTN.
- Živanović, B., Vidović, M., Milić Komić, S., Jovanović, L., Kolarž, P., Morina, F., & Veljović-Jovanović, S. (2017). Contents of phenolics and carotenoids in tomato grown under polytunnels with different UV-transmission rates. *Turkish Journal of Agriculture and Forestry*, 41, 113–120. <https://doi.org/10.3906/tar-1612-56>